Available online at www.sciencedirect.com
SCIENCE DIRECT®
Journal of Nuclear Materials 320 (2003) 126–132
journal of nuclear materials
www.elsevier.com/locate/jnucmat

# Irradiation behavior of rock-like oxide fuels

T. Yamashita [a,*], K. Kuramoto [a], N. Nitani [a], Y. Nakano [a], H. Akie [a], H. Nagashima [a], Y. Kimura [a], T. Ohmichi [b]

[a] Japan Atomic Energy Research Institute, Tokai, Ibaraki 319-1195, Japan
[b] Research Organization for Information Science and Technology, Tokai, Ibaraki 319-1195, Japan

**Abstract**

Two irradiation tests were performed on the rock-like oxide (ROX) fuels in order to clarify in-pile irradiation stabilities. In the first test small disk-shape fuel targets were irradiated in the JRR-3 in JAERI. In the second test pellet-type fuels were employed. Irradiation behaviors such as swelling, fractional fission gas release (FGR) and phase change were examined by puncture test, profilometry and ceramography. Swelling and FGR behavior of the pellet-type fuels improved considerably compared with the disk-type fuels. Yttria stabilized zirconia (YSZ) single-phase fuel showed an excellent irradiation behavior, i.e. low FGR (<3%), negligible swelling and no appreciable restructuring. The particle dispersed fuels showed lower swelling and higher FGR than those of mechanically blended fuels. Spinel decomposition and subsequence restructuring in the spinel matrix fuels was observed for the first time in the present investigation. It would be possible to reduce the FGR of the spinel matrix fuels to that of the corundum ones, if the maximum fuels temperature is limited below 1700 K where neither spinel decomposition nor restructuring was observed. Damaged area of spinel matrix due to fission fragment irradiation seemed to be confined to thin layers around the surface of YSZ particles as expected.


## 1. Introduction

In order to propose a new option for utilizing and annihilating so called excess plutonium, Japan Atomic Energy Research Institute (JAERI) has performed research on the plutonium rock-like oxide (ROX) fuels and their once-through burning in LWRs (the ROX-LWR system) [1,2]. The ROX-LWR system has the features capable of burning plutonium almost completely and disposing directly spent ROX fuels without reprocessing. The ROX fuel is multi-phase mixture of mineral-like compounds such as yttria stabilized zirconia (YSZ), spinel (SP: $MgAl_2O_4$) and corundum (CR: $Al_2O_3$), which are known to be very stable chemically and physically. Plutonium is incorporated in the YSZ phase forming a solid solution.

Irradiation stability of stabilized zirconia was demonstrated by Berman et al. [3] in in-pile irradiation experiments. They observed practically no changes in sample dimensions, density and microstructure for the calcia stabilized zirconia fuel of which composition was $ZrO_2$:CaO:$UO_2$ = 65.8:26.9:7.3 in mol%. However, its thermal conductivity is extremely low (~2 W/m K); less than one half of that of $UO_2$. Addition of SP or CR to YSZ may improve the total thermal conductivity. Indeed, measured thermal conductivity of a YSZ/SP composite (YSZ:$UO_2$:SP = 54.5:15.2:30.3 in mol%) was found to be similar to or slightly higher than that of $UO_2$ [4]. Irradiation stability of SP and CR was not as good as YSZ, especially for irradiation swelling. A new fuel design, a particle-dispersed fuel, was proposed to improve irradiation stability of these inert matrices [2,5]. In the case that appropriate size (100–250 μm) of YSZ particles were dispersed homogenously in the SP or CR

* Corresponding author. Tel.: +81-29 282 6951; fax: +81-29 282 5935.
*E-mail address:* yamasita@popsvr.tokai.jaeri.go.jp (T. Yamashita).

0022-3115/03/$ - see front matter 
doi:10.1016/S0022-3115(03)00178-8

matrix, damaged area of the matrix was limited to thin layers around the particle surfaces and the thermal conductivity of the whole fuel was expected to be maintained in almost the same value of the fresh fuel.

In-pile irradiation of inert matrix fuels or ROX fuels was very limited compared to $UO_2$ fuel. Much more information will be necessary to establish the irradiation behavior of these new fuels. Irradiation tests were performed in the Japan Research Reactor No. 3 (JRR-3) in JAERI in order to clarify the behavior of ROX fuels under irradiation. In the present paper, irradiation behavior such as swelling, fractional fission gas release (FGR) and microstructure change described are as obtained by post-irradiation examinations.

## 2. Experimental

### 2.1. Fabrication of fuel targets

Two types of fuel targets were fabricated for the irradiation tests in the JRR-3 in JAERI; one is a disk-shape specimen and the other is a pellet-shape one. Test fuel matrix and characteristics of the sintered fuels are listed in Table 1 and 2, respectively. Sample ZM is the disk-shape fuel and contains plutonium as fissile material. The other samples SD, SH, Z, CD and CH are the pellet-shape fuels where 20% enriched uranium is used as fissile material. The last column of Table 1 shows the fissile density of each fuel. The fissile density of conventional $UO_2$ fuel aimed at 45 $GW\,d\,t^{-1}$ burnup is about $10 \times 10^{20}$ $cm^{-3}$. These fuels have high values of fissile densities so as to yield high fission products in rather short irradiation periods (about 100 days). As can be seen from the last column of Table 2, the apparent densities of these fuels are about 90% TD except for the ZM and Z fuels. Detailed description of these disks and pellets were given elsewhere [5,6].

The ZM target was fabricated as follows: five disks separated by Nb/1 wt% Zr alloy sheets were loaded in a Nb/1 wt% Zr alloy case with an inner diameter of 4 mm and an outer diameter of 6 mm, sealed in a platinum sleeve and finally encapsulated in a Nb/1 wt% Zr alloy cladding with an inner diameter of 6.8 mm and an outer diameter of 10 mm, and 90 mm long. Both Pt-sleeve and Nb/1 wt% Zr cladding were filled with He gas. The rest of five targets with pellet-shape fuels were as follows: 10 pellets of each fuel were loaded into a stainless steel cladding tube of 6.50 mm outer diameter and of 5.56 mm inner diameter. He gas was added at ambient pressure as heat conductor. A fuel stack was about 55 mm long and total length of the fuel pin was 125 mm.

### 2.2. Irradiation

Three ZM targets were placed in a stainless steel irradiation capsule. Between the targets and the capsule case, aluminum blocks were used as heat conductor.

Table 1
Test fuel matrix

| Pin | Composition (mol%) | | | | | YSZ inclusion size | Fissile density ($10^{20}/cm^3$) |
|---|---|---|---|---|---|---|---|
| | YSZ[a] | $PuO_2$[b] | $UO_2$[c] | $MgAl_2O_4$ | $Al_2O_3$ | | |
| ZM | 16.7 | 11.1 | – | 11.1 | 61.1 | 2–10 μm | 21.10 |
| SD | 20.0 | – | 37.1 | 42.9 | – | 250 μm | 13.00 |
| SH | 20.0 | – | 37.1 | 42.9 | – | 10–50 μm | 13.10 |
| Z | 80.0 | – | 20.0 | – | – | Solid solution | 8.62 |
| CD | 16.5 | – | 30.6 | – | 52.9 | 250 μm | 13.54 |
| CH | 16.5 | – | 30.6 | – | 52.9 | 10–50 μm | 13.17 |

[a] YSZ = 79.9 mol% $ZrO_2$ + 20.1 mol% $YO_{1.5}$.
[b] Pu isotopic composition (at%) was 94.3, 5.3 and 0.4 for $^{239}Pu$, $^{240}Pu$ and $^{241}Pu$, respectively.
[c] 19.6% enriched $UO_2$.

Table 2
Characteristics of sintered fuels

| Pin | Diameter (mm) | Height (mm) | Density ($g\,cm^{-3}$) | Apparent density (%TD) |
|---|---|---|---|---|
| ZM | 3 | 1 | 4.3 | 81.6 |
| SD | $5.42 \pm 0.03$ | $5.54 \pm 0.28$ | $5.53 \pm 0.06$ | $90.6 \pm 1.0$ |
| SH | $5.35 \pm 0.02$ | $5.65 \pm 0.16$ | $5.57 \pm 0.03$ | $91.3 \pm 0.5$ |
| Z | $5.45 \pm 0.003$ | $5.55 \pm 0.27$ | $6.00 \pm 0.03$ | $85.7 \pm 0.4$ |
| CD | $5.46 \pm 0.01$ | $5.48 \pm 0.27$ | $5.89 \pm 0.07$ | $93.1 \pm 1.0$ |
| CH | $5.41 \pm 0.02$ | $5.65 \pm 0.27$ | $5.74 \pm 0.03$ | $90.6 \pm 0.5$ |

Table 3
Estimated irradiation conditions

| Pin | ZM-7 | ZM-6 | ZM-4 | | |
|---|---|---|---|---|---|
| Average power ($GW\,m^{-3}$) | 1.97 | 2.45 | 1.90 | | |
| Disk temperature (K) | $1040 \pm 50$ | $1270 \pm 10$ | $980 \pm 50$ | | |
| Burnup ($GW\,d\,m^{-3}$) | 192 | 237 | 184 | | |
| | SD | SH | Z | CD | CH |
| Linear power ($kW\,m^{-1}$) | 23.0 | 23.4 | 13.9 | 24.9 | 20.7 |
| Average power ($GW\,m^{-3}$) | 1.00 | 1.04 | 0.60 | 1.06 | 0.90 |
| Pellet surface temperature (K) | 1250 | 1440 | 990 | 1300 | 1290 |
| Pellet center temperature (K) | 1740 | 1940 | 1490 | 1820 | 1730 |
| Burnup ($GW\,d\,m^{-3}$) | 100 | 103 | 59 | 105 | 88 |

Irradiation was performed in an outer core region of JRR-3 during four reactor cycles (97 full power days). The neutron fluence was monitored using Al–Co wire flux monitors. Temperature of each target was measured by a thermocouple positioned close to the target. Irradiation temperature of the ZM-6 target was controlled at $1270 \pm 10$ K by changing composition and flow rate of $N_2$/Ne mixed gas passing through gaps between targets and aluminum blocks. This might result in slightly large variations of irradiation temperature for ZM-4 and ZM-7 targets.

A total of 5 targets, of which 2 targets contain spinel, 2 targets corundum and one target YSZ as an inert matrix, were placed in a stainless steel irradiation capsule. Aluminum blocks were used as heat conductor and all gaps were filled with $N_2$/Ne mixed gas. The outer surface of the irradiation capsule was cooled by cooling water of the JRR-3. These 5 targets were irradiated at nominal reactor power of 20 MW for four reactor cycles (100 full power days). The neutron fluence was monitored using Al–Co wire flux monitors. Temperature of each fuel target was measured by a thermocouple positioned close to the cladding.

Irradiation conditions were estimated by burnup analyses using the SRAC95 code system [7] referring to total neutron fluences which were determined by the fluence monitor analysis, and the results are summarized in Table 3. As can be seen from the table, all targets except for the ZM and Z targets were irradiated at remarkably high temperatures. Calculated burnups are indicated in the bottom row. The value of 100 $GW\,d\,m^{-3}$ is corresponding to nearly 10 $GW\,d\,t^{-1}$ of the conventional $UO_2$ fuel.

### 2.3. Post-irradiation examination

Post-irradiation examinations were performed at the Real Fuel Examination Facility in JAERI using following techniques: X-ray diffraction analysis (XRD), puncture test combined with mass spectrometry, metallography, scanning electron microanalysis (SEM) and electron probe microanalysis (EPMA). Irradiated fuel disks and pellets were embedded in a sample holder with epoxy resin, polished with diamond pastes and subjected to XRD, metallography, SEM and EPMA.

## 3. Results and discussion

### 3.1. Swelling

Few irradiated specimens of ZM targets kept their original circular disk shapes: some had large cracks and the others were broken into small pieces. The high average power density of 1.90–2.45 $GW\,m^{-3}$, which was estimated by burnup calculation, may have caused the fragmentation of the disks. Visual inspection by means of a low magnification telescope showed apparent volume increase and porous surface appearance. Because of the large cracks, it was impossible to determine precise sizes of the irradiated disks. Rough measurements showed that the diameter of the disk irradiated at 980 K (ZM-4) was about 3.6 mm and that of fresh fuel disks was about 3.25 mm; about 11% increase in diameter.

Pellet swelling due to irradiation was evaluated from changes in fuel stack lengths and diameters. Relative length of each fuel stack against total target length was determined from X-ray photos taken before and after irradiation. No stack elongation was observed for every target within the experimental error of 0.1 mm. The profilometry of each target showed that the diameter expansion was very small, less than 10 μm, except for the SH target where diameter increase of 60 μm was recorded at the maximum value. Diameter change ($\Delta\Phi$) was evaluated from the initial pellet diameter, a gap between the pellet and cladding, and profilometry value. Radial and volumetric swellings are summarized in the third and fourth column of Table 4. The radial swelling ($\Delta\Phi/\Phi$) is given by the ratio between the diameter change and the initial pellet diameter.

All pellet-type fuels showed smaller radial swelling than those of the ZM disk fuels. Disk fuel specimens might expand freely because almost no constraint was expected between the specimens and their sample cases. On the other hand, plenum springs and cladding tubes might put these pellets under tight constraint. The YSZ single phase fuel, Z target, shows the lowest swelling rate of 2.2%. The particle dispersed fuels, SD and CD targets, show lower swelling than the powder mixture fuels, SH and CH targets.

It should be noted that swelling of corundum-matrix fuels, CD and CH targets, was very small compared with the literature value of about 30% given by Berman et al. [3]. They irradiated the fuel specimen at low temperature (about 560 K) and found a large swelling due to amorphization of the corundum phase. In the present irradiation, on the other hand, central fuel temperature was estimated to be above about 1700 K. XRD analysis of the irradiated fuels clearly showed the existence of a crystalline corundum phase although some peak broadening were observed. The low swelling of corundum-matrix fuels may be attributed to rapid recovery from amorphous state due to high-irradiation temperature.

### 3.2. Fractional fission gas release

Gases in the fuel targets were collected and analyzed by means of a puncture test. The FGR of Xe is the ratio of the measured Xe volume and the calculated one which was obtained by the burnup analysis using the SRAC95 code, and the values are listed in the last column of Table 4. The burnup calculation showed that the Xe/Kr gas ratios were 18.1–18.3 and 7.2 for disk-type and pellet-type targets, respectively, which agreed well with the measured ratios of 17.3–18.0 and 7.0–7.2. Difference in the Xe/Kr ratio between the disk-type and pellet-type targets is due to the difference in the fissile materials; $^{239}Pu$ and $^{241}Pu$ for the disk-type fuels, and $^{235}U$ for the pellet-type fuels. Again, the Xe FRG for the pellet-type fuels improved very much compared to those of the disk-type fuels.

The YSZ single-phase fuel shows the lowest FGR of 2.2%. Contrary to the swelling behavior, the FGR of particle-dispersed fuels, SD and CD targets, is larger than that of the powder mixture fuels, SH and CH targets. The high FGR values indicate that the FP gas may release directly through open paths of hair cracks and not by diffusion through matrices. Such hair cracks may occur by the stress caused from a thermal expansion difference between the large YSZ fuel particles and matrices. A similar FGR behavior was reported recently by Bakker et al. [8] and Neeft et al. [9]. They observed higher FGR for the 'macro' dispersed fuels, where large fissile inclusions of diameter about 150 μm were dispersed in spinel matrix, than the 'micro' dispersed ones of which typical fissile inclusion size was less than 1 μm. In order to reduce the FGR of the particle-dispersed fuels, sintering condition and procedure for the fuel fabrication must be improved to obtain fuel pellets with the optimum sintered density and with gaps between the particle and spinel matrix so that hair crack generation can be suppressed during irradiation.

### 3.3. Microstructure change

Fig. 1 shows SEM images of un-irradiated, ZM-7 and ZM-6 fuels. These images were taken at the central part of disks. In the irradiated fuel small grains of fluorite (gray), hibonite (dark gray) and corundum/spinel (black) phases are distributed homogeneously. In the irradiated ZM-7 disk some agglomerates of corundum are observed, and size and number of pores do not increase appreciably compared with the un-irradiated fuel. On the other hand, large pores and grains of the fluorite phase are observed in the irradiated ZM-6 disk. Porosity of the ZM-6 disk is deduced to be 45.4% from the graphics treatment of the SEM image. Formation of hibonite phases in corundum phase is also clearly observed. The general formula of the hibonite phase was given as $LnM^{2+}Al_{11}O_{19}$ by Gasperin et al. [10], where Ln = lanthanide elements and $M^{2+}$ = divalent cations such as alkaline earths, Mn, Fe, Co, Ni, Cu. Alkaline earths and lanthanides in fission products and trivalent actinides could be immobilized by making hibonite phases.

Table 4
Dimensional variation and fractional gas release of ROX fuels

| Pin | Maximum temperature (K) | $\Delta\Phi/\Phi$ (%) | $\Delta V/V$ (%) | Xe FGR (%) |
|---|---|---|---|---|
| ZM-7 | 1040 | – | – | 63 |
| ZM-6 | 1270 | – | – | 61 |
| ZM-4 | 980 | 10.8 | – | 63 |
| SD | 1850 | 2.7 | 5.5 | 38 |
| SH | 2080 | 5.0 | 10.2 | 22 |
| Z | 1580 | 2.0 | <4.0 | 2.2 |
| CD | 1930 | 2.1 | 4.3 | 22 |
| CH | 1830 | 2.8 | 5.7 | 7.8 |

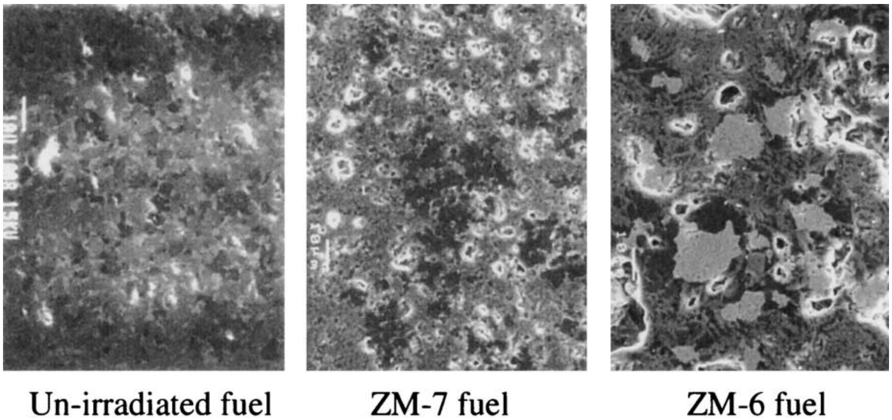


Fig. 1. Microstructures of ZM fuels obtained by SEM. Left: un-irradiated fuel; middle: ZM-7, irradiated at 1040 K; right: ZM-6, irradiated at 1270 K.

At the peripheral region of the ZM-6 disk no appreciable grain growth was observed but a large grain growth was clearly observed at the intermediate and central regions. This indicates that there existed a thermal gradient across the disk to some extent. However, the temperature of the central region of the disk might not have been very high, because spinel decomposition and subsequent phase restructuring were not observed as described in the following paragraph.

Ceramographic photos of the cross-sections of irradiated Z, SH and CH fuels are shown in Fig. 2. Several large radial cracks are observed in all fuels as also observed in the conventional irradiated $UO_2$ fuel. No apparent microstructure change was recognized in the Z and CH fuels. On the other hand, a significant structure change is observed in the SH fuels mainly in the central region. Such a structure change in spinel matrix fuel was observed for the first time in the present irradiation experiment. A precise SEM image of the SH fuel is shown in Fig. 3 together with existing phases analyzed by EPMA. A hole of about one mm in diameter was formed in the center of the pellet. A bright region (I) around the central hole was found to be YSZ phase containing uranium. An outer ring region (II) of about 0.5 mm thick around the YSZ region consisted of YSZ and corundum phases. Most outer region (III) was a mixture of YSZ and spinel and its microstructure was nearly the same as that of a fresh fuel. The temperature between regions (II) and (III) was calculated to be about 1700 K assuming the initial thermal conductivities of matrices. In the region below 1700 K, neither spinel decomposition nor restructuring was observed.

Spinel may decompose to $Al_2O_3$ and MgO by heavy fission fragment irradiation. Above 1700 K and under high thermal gradient (2000 $K\,cm^{-1}$), MgO vaporized incongruently from the spinel matrix and transported to a cooler region because the vapor pressure of MgO was higher by about 5 orders of magnitude than that of $Al_2O_3$. Vaporization of MgO and subsequent restructuring may be a driving force of the central hole formation by pushing closed pores in the matrix to the center. This restructuring seems to be one of possible reasons to yield the high FGR of spinel matrix fuels compared with that of the corundum matrix fuels where appreciable microstructure change was not observed.

Fig. 4 shows SEM images and main element maps obtained by EPMA near a YSZ particle at outer region

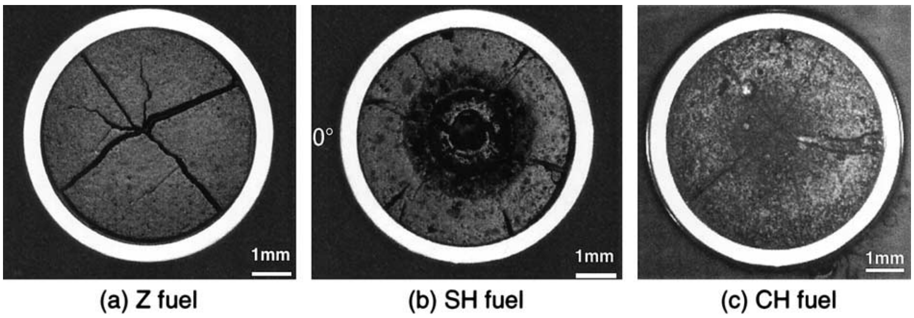


Fig. 2. Cross-sectional views of irradiated Z, SH and CH fuels.

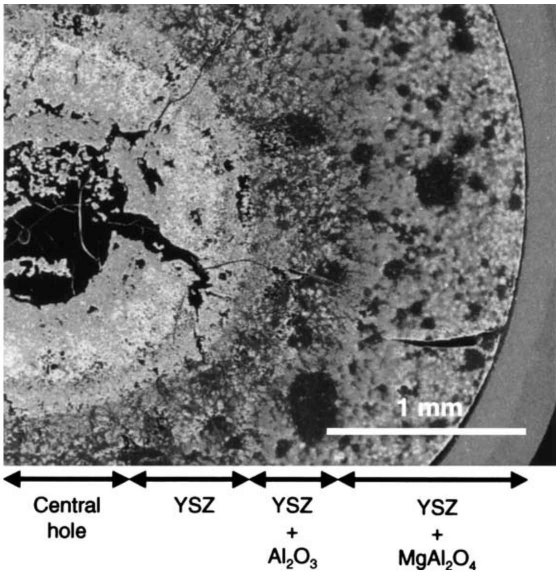


Fig. 3. SEM image of the irradiated SH fuel. Phases identified by EPMA were indicated below the figure. MgO was observed on the inner surface of the cladding.

of the SD fuel. Surface layer of the YSZ particle changes its color to dark. This layer is about 5 μm thick and almost corresponds to the fission fragment ranges. Element maps show that both YSZ and SP ($MgAl_2O_4$) exist in this layer. The formation of this layer might be the direct consequence of the reaction between YSZ and damaged SP matrix by fission fragment irradiation, and gives a clear evidence for the limitation of damaged area of SP matrix to the surface near a YSZ particle. Neeft et al. also reported that the fission gas bubbles were localized in a thin layer (6.5–14 μm) of matrices around $UO_2$ inclusions [9].

## 4. Conclusions

Two irradiation tests were performed for a disk-type and pellet-type ROX fuels in the JRR-3 in JAERI in order to clarify the irradiation behavior such as swelling, fractional FGR and microstructure change. Swelling and FGR behavior of the pellet-type fuels improved considerably compared with the disk-type fuels.

The particle dispersed fuels showed a behavior with low swelling as expected from their design. However, they showed higher FGR than those of powder mixture fuels. Because a mismatch in thermal expansion between an YSZ particle and spinel matrix would cause hair cracks and the resultant high FGR, further improvements must be carried out for the fuel fabrication technologies, especially sintering conditions, to reduce the FGR. Optimization of a sintered pellet density and a

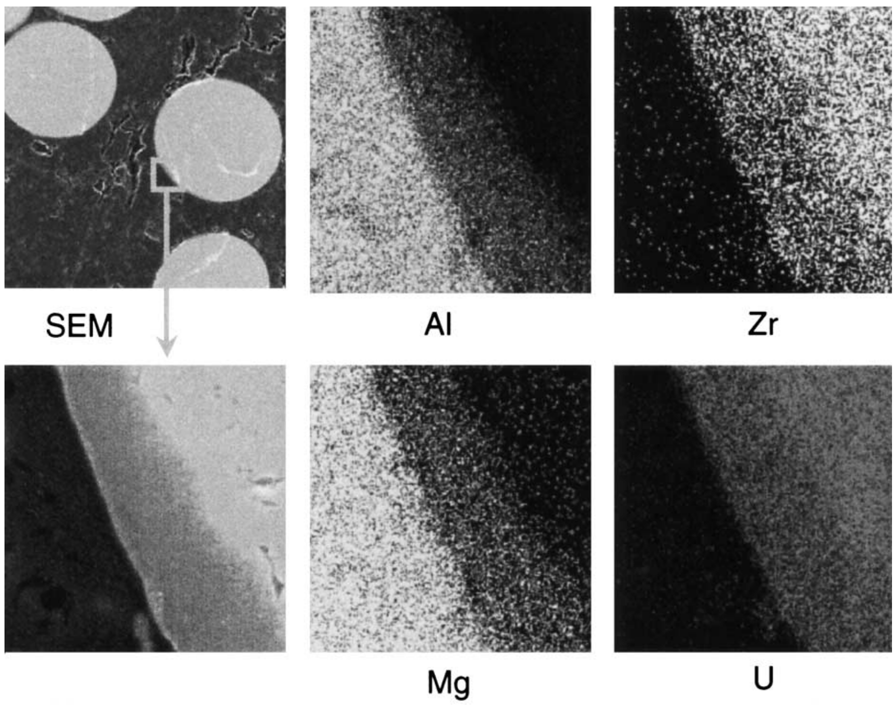


Fig. 4. SEM images and main element mappings obtained by EPMA near a YSZ particle at outer region of the SD fuel. Element mappings are shown such element as Al, Zr, Mg and U. White indicates high yield of the element while black none.

tailored gap width between YSZ particles and spinel matrix will be the key for that improvement.

Spinel decomposition and subsequence restructuring in the spinel matrix fuels was observed for the first time in the present investigation probably due to very high irradiation temperatures. This restructuring might be one of possible reasons to result in a high FGR of spinel matrix fuels compared with the corundum matrix fuels. However, it would be possible to reduce the FGR of the spinel matrix fuels to that of the corundum ones, if the maximum fuels temperature is limited below 1700 K where neither spinel decomposition nor restructuring was observed.

Damaged area of spinel matrix due to fission fragment irradiation seemed to be confined to thin layers around the surface of YSZ particles as expected.

## References

[1] H. Akie, T. Muromura, H. Takano, S. Matsuura, Nucl. Technol. 107 (1994) 182.
[2] T. Yamashita, K. Kuramoto, H. Akie, Y. Nakano, N. Nitani, T. Nakamura, K. Kusagaya, T. Ohmichi, J. Nucl. Sci. Technol. 39 (2002) 865.
[3] R.M. Berman, M.I. Bleiberg, W. Yeniscavich, J. Nucl. Mater. 2 (1960) 129.
[4] N. Nitani, T. Yamashita, T. Matsuda, S. Kobayashi, T. Ohmichi, J. Nucl. Mater. 274 (1999) 15.
[5] T. Shiratori, T. Yamashita, T. Ohmichi, A. Yasuda, K. Watarumi, J. Nucl. Mater. 274 (1999) 40.
[6] T. Yamashita, N. Nitani, H. Kanazawa, M. Magara, T. Ohmichi, H. Takano, T. Muromura, J. Nucl. Mater. 274 (1999) 98.
[7] K. Okumura, K. Kaneko, K. Tsuchihashi, Japan Atomic Energy Research Institute Report JAERI-Data/Code 96-015, 1996 (in Japanese).
[8] K. Bakker, R. Belvroy, F.A. van den Berg, S. Casalta, R. Conrad, E.A.C. Neeft, R.P.C. Schram, W. Tams, Prog. Nucl. Energy 38 (2001) 313.
[9] E.A.C. Neeft, K. Bakker, H.A. Buurveld, J. Minkema, A. Paardekooper, R.P.C. Schram, C. Sciolla, O. Zwaagstra, B. Beemsterboer, J.R.W. Woittiez, P. van Vlaanderen, W.J. Tams, H. Hein, R. Conrad, A. van Veen, Prog. Nucl. Energy 38 (2001) 427.
[10] M. Gasperin, M.C. Saine, A. Kahn, F. Laville, A.M. Lejus, J. Solid State Chem. 54 (1984) 61.